Progress of Theoretical Physics, Vol. 77, No. 1, January 1987

Suppression of Off-Energy-Shell Interaction in Nuclear 3-, 4- and ∞-Body Systems

Isamu ARISAKA, Toshiyuki KATAYAMA*,
Kimiko NAKAGAWA** and Toshio OBINATA**

Department of Physics, Chiba Institute of Technology
Narashino 275
**Department of Physics, Hokkaido University, Sapporo 060*
***Physical Science Laboratories, College of Science and Technology*
Nihon University, Funabashi 274

(Received July 9, 1986)

The binding energies of ^{3}H and ^{4}He are calculated with two kinds of the Funabashi potential. These potentials, which have been so constructed as to be nearly phase-equivalent ones, differ with each other in the off-energy-shell interaction coming from the retardation of meson exchange process and in the strength of tensor force. Comparing the calculated results with the binding properties of deuteron and nuclear matter for the same potentials, it is found that both effects of the off-energy-shell interaction and the tensor force are increasingly suppressed as the mass number becomes larger.

§ 1. Introduction

Many theoretical works on few-nucleon systems have shown that realistic N-N potentials, which reproduce the low energy two-nucleon data, give underbindings by 1~2 MeV to ^{3}H and by 5~7 MeV to ^{4}He.[1] The shortage of binding energies is usually attributed to such sources as the three-body force, relativistic corrections and the uncertainty of N-N interaction itself. However, our knowledge about the contributions from these sources is far from the satisfactory one.

The variational calculations[2a),3)] have shown that the Fujita-Miyazawa type three-body force[4] produced additional bindings by 1~1.5 MeV in ^{3}H and by 6~12 MeV in ^{4}He. Taking this force into account, we are faced with the situation in which ^{3}H is slightly underbound but ^{4}He becomes overbinding by a few MeV.

Relativistic corrections to ^{3}H were estimated to give an additional binding by 0.5~1 MeV,[5] while the corrections to ^{4}He are not clear.

As concerns N-N potentials, some kinds of uncertainty remain unresolved. The following two are serious problems for nuclear structure calculations. One is the uncertainty of off-energy-shell (OES) interaction and the other is related to the strength of tensor force in the triplet-even state. The change of the OES behavior of N-N interaction produced an additional binding by at most 0.5 MeV in the ^{3}H system,[6] while the effect on ^{4}He is poorly understood. The tensor force uncertainty, which originates in the undecided experimental D-state probability of the deuteron, is anticipated having a relatively large influence on the binding properties of few-nucleon systems. In studying the nuclear matter, the fact that N-N potentials with strong tensor force predict less binding energies, has been well known and called the tensor suppression. But a detailed discussion on the tensor contribution to few-

nucleon systems has not yet been done.

Under these circumstances, it is important to clarify the systematic trend of contributions from the sources mentioned above to the binding properties extending over different nuclei.

The purpose of this paper is to estimate both effects of the OES interaction and the tensor force on ^{3}H and ^{4}He, and to clarify their mass number dependence by comparing them with the same effects on the deuteron and the nuclear matter.

Through this work, it is found that both effects of the OES interaction and the tensor force on binding properties decrease with increase of the mass number.

We perform the calculations for ^{3}H and ^{4}He variationally by using the ATMS method[2] which enable us to treat simultaneously the three- and four-nucleon systems on the same footing. As realistic N-N potentials we employ two kinds of the r-space Funabashi potentials.[7),8)] The binding energies[8)] of the deuteron and the nuclear matter with the same potentials are compared with the results of ^{3}H and ^{4}He calculated here.

In § 2, the ATMS method and the Funabashi potentials are briefly summarized. Variational parameters and numerical methods for the ATMS are mentioned in § 3. In § 4, the calculated results for ^{3}H and ^{4}He are presented and compared with the results for the deuteron and the nuclear matter. A summary and a conclusion are stated in § 5.

§ 2. The ATMS method*) and the Funabashi potentials

2.1 *The ATMS method*

Whether we succeed or not in variational calculations depends on how to construct a trial function Ψ of the system. In the ATMS method, Ψ is constructed through three steps and given in the form:

$$\Psi = F\Phi\,, \tag{1}$$

where Φ is an initial wave function and F is a total correlation function.

The first step is to set up Φ so as to describe symmetric properties of the system and the correct asymptotic behavior of Ψ.

In the second step, two-body correlation functions are dynamically determined. First, the initial two-body function $\varphi(ij)$ for the ^{3}H case is squeezed from Φ as follows:

$$\varphi(ij)\equiv\varphi(r)=\left[\int d\hat{\boldsymbol{r}}\int d\boldsymbol{\rho}\,|\Phi(\boldsymbol{r},\boldsymbol{\rho})|^2\right]^{1/2}, \tag{2}$$

where $\boldsymbol{r}=\boldsymbol{r}_i-\boldsymbol{r}_j$ and $\boldsymbol{\rho}=\boldsymbol{r}_k-(\boldsymbol{r}_i+\boldsymbol{r}_j)/2$. Then we solve the reaction matrix equation for the (ij)-pair,

$$\psi(ij)=\varphi(ij)+\frac{Q_{ij}}{e}v(ij)\psi(ij)\,, \tag{3}$$

$$v(ij)\psi(ij)=g_{ij}\varphi(ij)\,, \tag{4}$$

*) Although, at present, the Hokkaido University group is reconstructing the ATMS as an exact theory, we adopt here the ordinary ATMS.

where $v(ij)$ is the N-N potential, g_{ij} the reaction matrix, $Q_{ij}=1-|\varphi(ij)\rangle\langle\varphi(ij)|$, $e=E_M-H_M$, $E_M=\langle\Phi|H_M|\Phi\rangle$ and

$$H_M=-\frac{\hbar^2}{2M}\sum_{i=1}^{A}\nabla_i^2+\frac{\hbar^2}{2AM}(\sum_{i=1}^{A}\nabla_i)^2+\sum_{(ij)}g_{ij}(1-Q_{ij})\,.$$

Using the solution of Eq. (3), we approximate the operator $(Q_{ij}/e)g_{ij}$ by two kinds of the two-body correlation function as follows:

$$\frac{Q_{ij}}{e}g_{ij}=-\{\varphi(ij)-\psi(ij)\}/\varphi(ij)$$

$$=\begin{cases}-\eta(ij) & \text{for on-shell}\,,\\ -\zeta(ij) & \text{for off-shell}\,.\end{cases} \tag{5}$$

Practically, $\zeta(ij)$ is constructed by modifying $\eta(ij)$ as shown in Eq. (16) or Eq. (20).

In the last step, we use $\eta(ij)$ and $\zeta(ij)$ instead of $(Q_{ij}/e)g_{ij}$ in the equation of multiple scattering operator,

$$\hat{F}=1+\sum_{(ij)}\frac{Q_{ij}}{e}g_{ij}\hat{F}_{ij}\,, \tag{6}$$

$$\hat{F}_{ij}=1+\sum_{(kl)\neq(ij)}\frac{Q_{kl}}{e}g_{kl}\hat{F}_{kl}\,. \tag{7}$$

We get finally a functional,

$$F=F(\eta,\zeta)\,. \tag{8}$$

This is the total correlation function F appeared in Eq. (1).

A few parameters introduced in each step are varied to minimize the expectation value of the Hamiltonian for the system. The derivation of trial function in this manner is so skilful that the detail analysis of the contributions from each part of the N-N potential is possible. More details for the ATMS method are found in Ref. 2).

2.2 *The Funabashi potentials*

In the p-space, a one-boson-exchange potential (OBEP) with retardation is written as

$$U(\boldsymbol{p}',\boldsymbol{p})=-\sum_{\alpha}[\bar{u}(\boldsymbol{p}')\Gamma_\alpha u(\boldsymbol{p})][\bar{u}(-\boldsymbol{p}')\Gamma_\alpha u(-\boldsymbol{p})]\bar{\Delta}_\alpha(\boldsymbol{k}^2)\,, \tag{9}$$

where $\bar{\Delta}_\alpha(\boldsymbol{k}^2)=P/\{m_\alpha^2+\boldsymbol{k}^2-(E'-E)^2\}$, $\boldsymbol{k}=\boldsymbol{p}'-\boldsymbol{p}$, the suffix α stands for the exchanged meson, $u(\boldsymbol{p})$ is the Dirac spinor, Γ_α a covariant operator describing the meson-nucleon vertex and m_α the meson mass. Ignoring the OES term $(E'-E)^2$ in $\bar{\Delta}_\alpha(\boldsymbol{k}^2)$, we get the usual Yukawa potential, i.e., the OBEP without retardation. Here it should be noted that the retardation is essentially an OES interaction.

To get the r-space OBEP, we expand $U(\boldsymbol{p}',\boldsymbol{p})$ up to the order of $O(\boldsymbol{p}^2/M)$, where M is the nucleon mass, and perform the Fourier transformation. In this process, the meson propagator $\bar{\Delta}_\alpha(\boldsymbol{k}^2)$ is also approximated as

$$\bar{\Delta}_a(\boldsymbol{k}^2)\cong\frac{1}{\boldsymbol{k}^2+m_a{}^2}+\frac{(E'-E)^2}{(\boldsymbol{k}^2+m_a{}^2)^2}\,. \tag{10}$$

Corresponding to this approximation, the r-space OBEP has the form:

$$v=V+W\,, \tag{11}$$

where V is the OBEP without retardation and W the retarded one.

The N-N potentials used in this study are two kinds of the nonstatic r-space OBEP called the Funabashi potentials;[7),8)] that is OBEG(R) and OBEG(NR) (hereafter abbreviated as (R) and (NR) likewise Ref. 8)). Both potentials (R) and (NR) have a common soft core with the Gaussian type, while (R) includes the retarded part W of Eq. (11) but (NR) does not. The meson-nucleon coupling constants of both (R) and (NR) are determined so as to reproduce the low energy two-nucleon data. Namely, (R) and (NR) are nearly phase-equivalent potentials. Remarkable differences between the two are in the OES behavior caused by the retardation and in the strength of tensor force in the triplet-even state; the tensor force of (R) is stronger than that of (NR). In addition, it should be noted that the effect of the retarded part is attractive in the two-nucleon system and the nuclear matter.[7),8)]

§ 3. The ATMS calculations for ^{3}H and ^{4}He

Our procedures for the ATMS calculations are the same as those of Refs. 2b) and 2c). Here, we mention the variational parameters and the numerical methods briefly for consistency.

3.1. *The variational parameters for* ^3H

In the case of ^{3}H, the initial wave function Φ in Eq. (1) is taken to be

$$\Phi=\Phi_S\{T=1/2,\,S=1/2\}_A\,, \tag{12}$$

where $\{T,\,S\}_A$ is an antisymmetric isospin-spin function and Φ_S is a symmetric spatial function of interparticle distance $r_{ij}=|\boldsymbol{r}_i-\boldsymbol{r}_j|$ only. And the function Φ_S is given as

$$\Phi_S=\prod_{(ij)}f(r_{ij}) \qquad ;\ (i,j=1,2,3)\,, \tag{13}$$

$$f(r)=N\begin{cases}\exp(-\beta r^2/6) & ;r\leqq r_0\,,\\ Ar^{1/2}\exp(-\alpha r/2) & ;r>r_0\,,\end{cases} \tag{14}$$

where r_0 and A are determined so that $f(r)$ and its derivative are continuous at r_0. The constants α and β are related to the separation energy $E_S=3\hbar^2\alpha^2/4M$ and the harmonic oscillator energy $\hbar\omega=\hbar^2\beta/M$, respectively. For the case of ^{3}H, E_S is fixed to 4 MeV, while $\hbar\omega$ is adopted as a variational parameter.

The on-shell correlation function η obtained by Eq. (5) has the form:

$$\eta(ij)={}^1\eta_S(r_{ij})P^{1E}(ij)+{}^3\eta_S(r_{ij})P^{3E}(ij)+{}^3\eta_D(r_{ij})S_{ij}P^{3E}(ij)\,, \tag{15}$$

where $P^{1E}(ij)$ and $P^{3E}(ij)$ are projection operators to the singlet-even and the triplet-even state, respectively, and S_{ij} is the tensor operator for the (ij)-pair. As the

off-shell correlation function ζ, we assume the following form:

$$\zeta(ij)=\{{}^3\eta_S(r_{ij})+m_D{}^3\eta_D(r_{ij})\}\exp(-ar_{ij}^2)\,, \tag{16}$$

where m_D and a are the variational parameters. We introduce further two parameters, a_3 and a_1. In constructing F, $(1-{}^3\eta_S)$ and ${}^3\eta_D$ are multiplied by a_3 and $(1-{}^1\eta_S)$ by a_1. In addition to these, the starting energy E_M that is used for solving Eq. (3) and the harmonic oscillator energy $\hbar\omega_0$ which is used for Φ in Eq. (2), are varied in the variational process. Therefore, variational parameters are the following seven; $\hbar\omega$, m_D, a, a_3, a_1, E_M and $\hbar\omega_0$.

3.2. *The variational parameters for* ^{4}*He*

For the case of ^{4}He, Φ is taken to be

$$\Phi=\Phi_S\{T=0, S=0\}_A\,, \tag{17}$$

$$\Phi_S=\prod_{(ij)} f(r_{ij}) \qquad ;(i,j=1,2,3,4)\,, \tag{18}$$

$$f(r)=N\begin{cases}\exp(-\beta r^2/8) & ;r\leqq r_0\,,\\ Ar^{1/2}\exp(-ar/3) & ;r>r_0\,.\end{cases} \tag{19}$$

The separation energy $E_S=2\hbar^2\alpha^2/3M$ is fixed to 100 MeV and $\hbar\omega=\hbar^2\beta/M$ is a variational parameter similar to the ^{3}H case. For ζ, we assume the form:

$$\zeta(ij)={}^1\eta_S\exp(-ar_{ij}^2)\,, \tag{20}$$

where a is a variational parameter. The starting energy E_M for Eq. (3) is determined self-consistently. The others are the same as those of the ^{3}H case. The five parameters, $\hbar\omega$, a, a_3, a_1 and $\hbar\omega_0$ are varied in the calculation of ^{4}He.

3.3. *Numerical methods*

To evaluate physical quantities, it is necessary to perform numerically three-fold integrations for ^{3}H and nine-fold ones for ^{4}He. All integrands are written by the interparticle distance r_{ij} whose domain is $[0,\infty]$. In the practical evaluations, r_{ij} is transformed into x_{ij} as follows:

$$x_{ij}=1-\exp(-r_{ij}/A_C)\,, \tag{21}$$

so the integral domain changes from $[0,\infty]$ to $[0,1]$. In the case of ^{3}H, the integrations over x_{12} and x_{23} are carried out by Simpson's formula with 1/80 mesh size, while that over x_{31}, final integration is done by the Gaussian 30-point quadrature formula. Integrations in the case of ^{4}He are carried out by the quasi-random-number method.[2d] The range constant A_C in Eq. (21) is fixed to 3.5 fm for ^{3}H and 4.0 fm for ^{4}He.

Details of the numerical accuracy are summarized in Ref. 9).

§ 4. Results and discussion

4.1. *Binding energies of* ${}^3H$ *and* ${}^4He$

Parameters mentioned above are varied to minimize the expectation value of the

Hamiltonian,

$$H=-\frac{\hbar^2}{2M}\sum_{i=1}^{A}\nabla_i^2+\frac{\hbar^2}{2AM}(\sum_{i=1}^{A}\nabla_i)^2+\sum_{(ij)}v(ij)\,, \tag{22}$$

where $A=3$ for ^{3}H and $A=4$ for ^{4}He, and $v(ij)$ is (R) or (NR).

In order to examine the OES contributions, we perform further calculations with a modified potential (R)′ which is the same as (R) except for only one point: The retarded part is multiplied by the factor 0.8.

Resulting energies of ^{3}H are -6.30 MeV for (NR) and -6.60 MeV for (R) and -4.33 MeV for (R)′. And energies of ^{4}He are -22.19 MeV for (NR), -20.37 MeV for (R) and -16.00 MeV for (R)′. The values of variational parameters producing these results are listed in Table I. Curves of the upper-bound energy versus r.m.s. radius are illustrated in Fig. 1 for ^{3}H and in Fig. 2 for ^{4}He, which are obtained by varying the parameter $\hbar\omega$ but keeping the others to the values of Table I. In Fig. 3, similar curves for the nuclear matter[8] calculated by the lowest order Brueckner theory with (R) and (NR) are shown for comparison. Both potentials (R) and (NR) give underbindings to ^{3}H and ^{4}He, likewise other realistic N-N potentials. It should be noted in Figs. 1~3 that the binding energy of ^{3}H with (R) is larger than that with (NR), while the roles of potentials are reversed in both cases of ^{4}He and the nuclear matter. The reversal occurring between ^{3}H and ^{4}He seems to be inconsistent with the Tjon line which stands for the linearity appeared in the calculated energies of ^{3}H and

Table I. The values of variational parameters at the minimum points.

Nucleus	^{3}H			^{4}He		
Potential	(NR)	(R)	(R)′	(NR)	(R)	(R)′
$\hbar\omega_0$(MeV)	16	16	16	22	21	21
E_M(MeV)	18	21	15	—	—	—
$\hbar\omega$(MeV)	15.5	16.7	16.0	15.2	14.4	14.0
a(fm^{-2})	0.2	0.6	0.6	0.6	0.6	0.6
m_D	-0.65	-0.80	-0.85	—	—	—
a_3	1.50	1.45	1.50	1.2	1.2	1.2
a_1	0.95	0.95	1.07	1.0	1.0	1.0

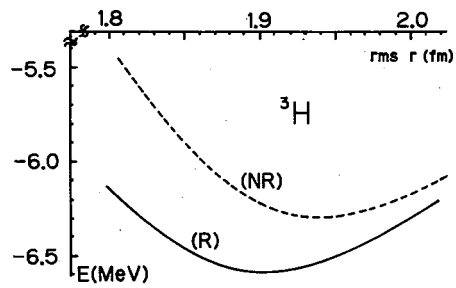

Fig. 1. The energy versus r.m.s radius for ^{3}H calculated by (R)(solid line) and (NR)(dashed line).

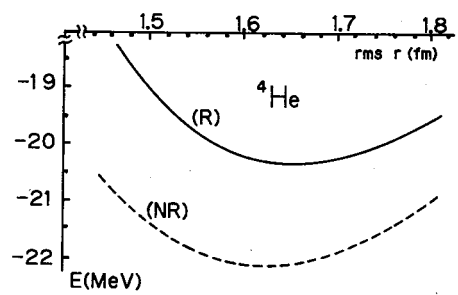

Fig. 2. Same as in Fig. 1, but for ^{4}He.

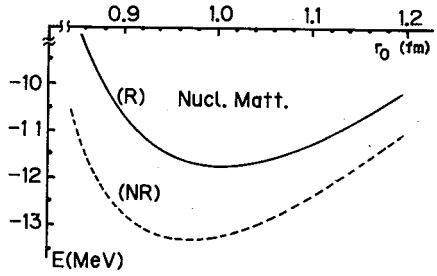

Fig. 3. The energy versus nuclear radius parameter r_0 for the nuclear matter calculated by (R)(solid line) and (NR)(dashed line).

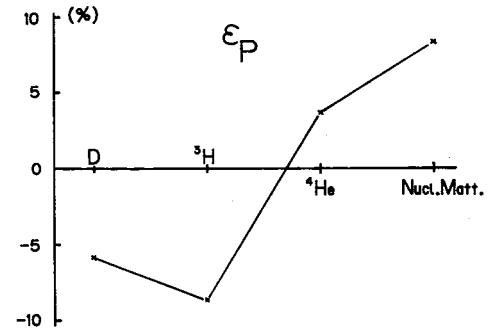

Fig. 4. The mass number dependence of the ratio ε_P (given by Eq. (23) in the text).

^{4}He with many types of N-N potential.

To clarify the cause for this reversal is the main theme of this study. To this end, we examine the interaction energy itself and the contributions from the retardation and the tensor force.

4.2. *Mass number dependence of interaction energies*

In order to investigate the origin of the reversal, we introduce a ratio given by

$$\varepsilon_P=\{\langle\Psi|v|\Psi\rangle_{(R)}-\langle\Psi|v|\Psi\rangle_{(NR)}\}/|\langle\Psi|v|\Psi\rangle_{(R)}|\,, \tag{23}$$

where $\langle\Psi|v|\Psi\rangle_{(R)}$ and $\langle\Psi|v|\Psi\rangle_{(NR)}$ stand for the interaction energies with (R) and (NR), respectively. The ratio for each nucleus is shown in Fig. 4. In Fig. 4, the interesting features of (R) and (NR) are shown. For the deuteron and ^{3}H, the ratios are -6.29% and -8.79%, respectively. To the contrary, those of ^{4}He and the nuclear matter are 3.67% and 8.43%, respectively. The negative sign of the ratio means that (R) is more attractive than (NR). Then the attractive behavior of (R) is stronger than that of (NR) in the deuteron and ^{3}H. This behavior is reversed in ^{4}He and the nuclear matter. According to this fact, it is clear that this change of sign occurred between ^{3}H and ^{4}He just corresponds to the reversal appeared in the binding energy. Namely, the reversal in binding energy is owing to the interaction energy itself.

4.3. *Contributions from the retardation and the tensor force*

The characteristic differences between (R) and (NR) are in the retardation and the strength of tensor force in the triplet-even state. Here we estimate how these differences affect the binding properties of the deuteron, ^{3}H, ^{4}He and the nuclear matter.

The contents of energies of ^{3}H and ^{4}He are given in Table II. Details of energies[8] of the deuteron and the nuclear matter are given in Tables III and IV.

Comparing (R) with (R)′, we can see from Table II that the retarded potential has attractive contributions to ^{3}H and ^{4}He, likewise the cases of the two-nucleon system and the nuclear matter. Let us consider a ratio,

$$\varepsilon_R=\{\langle\Psi|v|\Psi\rangle_{(R)}-\langle\Psi|v|\Psi\rangle_{(R)'}\}/\langle\Psi|v|\Psi\rangle_{(R)}\,, \tag{24}$$

Table II. Details of energies of ^{3}H and ^{4}He, where 1E, 3E, 1O and 3O stand for the singlet-even, triplet-even, singlet-odd and triplet-odd states, respectively.

(in MeV)

Nucleus	^{3}H			^{4}He		
Potential	(NR)	(R)	(R)′	(NR)	(R)	(R)′
Total E.	−6.30	−6.60	−4.33	−22.19	−20.37	−16.00
Kin. E.	37.09	40.97	35.00	70.74	69.27	63.81
S-state	25.70	25.92	22.80	48.91	44.52	41.77
D-state	11.39	15.05	12.20	21.83	24.75	22.04
Int. E.	−43.39	−47.57	−39.33	−92.93	−89.64	−79.81
V_C(1E)	−11.52	−11.38	−10.00	−28.48	−26.06	−23.78
V_C(3E)	−4.96	2.15	1.73	−11.19	3.21	3.20
V_C(1O)	0.01	0.01	0.01	0.01	0.01	0.01
V_C(3O)	0.07	0.14	0.07	0.50	0.76	0.55
V_T(3E)	−26.22	−38.50	−31.25	−51.70	−67.91	−60.02
V_T(3O)	−0.11	−0.14	−0.11	−0.41	−0.49	−0.46
V_{LS}	−0.61	0.78	0.58	−0.77	1.52	1.27
V_{QLS}	−0.05	−0.63	−0.36	−0.87	−0.68	−0.58
rms r(fm)	1.94	1.90	2.01	1.62	1.66	1.71
P_S(%)	93.1	92.0	92.9	90.0	89.1	89.6
$P_{S'}$(%)	0.6	0.5	0.3	0.1	0.2	0.1
P_D(%)	6.4	7.5	6.8	9.9	10.7	10.3

Table III. Deuteron energies.

(in MeV)

Potential	(NR)	(R)	(R)′
Total E.	−2.225	−2.224	−1.329
Kin. E.	18.842	20.258	15.211
S-state	10.989	10.989	8.331
D-state	7.853	9.359	6.880
Int. E.	−21.067	−22.482	−16.540
V_C(3E)	−2.995	1.012	0.745
V_T(3E)	−17.284	−23.696	−17.415
V_{LS}(3E)	−0.462	0.441	0.302
V_{QLS}(3E)	−0.326	−0.239	−0.172
P_S(%)	94.428	93.875	95.010
P_D(%)	5.572	6.125	4.990

where $\langle \Psi | v | \Psi \rangle_{(R)}$ and $\langle \Psi | v | \Psi \rangle_{(R)'}$ stand for the interaction energies with (R) and (R)′, respectively. The retarded part of (R)′ is weaker than that of (R) by 20%. Then the ratio ε_R represents the effect of the weakened retardation, viz., the difference in the OES interaction. In Fig. 5, the ratio for each nucleus is illustrated and we can see a systematic trend that the ratio decreases in order of the deuteron, ^{3}H and ^{4}He. Namely, at least, in light nuclei the OES contribution caused by the retardation decreases with increase of the mass number; the suppression of the OES interaction

Table IV. Partial wave contributions to the total energy of nuclear matter at the saturation point.

(in MeV)

Potential	(NR)	(R)	(R)′
Total E.	−13.34	−11.78	−8.70
Kin. E.	31.05	29.16	25.78
Int. E.	−44.39	−40.94	−34.48
(Tensor)[a]	(−17.88)	(−27.06)	(−23.41)
$^1S_0$	−20.87	−20.23	−17.02
$^1P_1$	5.91	4.97	4.09
$^1D_2$	−4.42	−3.51	−2.71
$^3S_1$	−19.59	−17.75	−15.21
$^3D_1$	2.63	2.32	1.80
$^3D_2$	−7.34	−6.00	−4.69
$^3D_3$	0.45	0.49	0.38
$^3P_0$	−5.94	−5.59	−4.78
$^3P_1$	16.96	15.14	12.10
$^3P_2$	−12.18	−10.78	−8.44
r_0(fm)	0.964	0.996	1.058
Total x[b]	0.113	0.116	0.112

a) Total contribution from the tensor forces.
b) Total wound integral.

increases as the mass number becomes larger. Hereafter this suppression is referred to as the OES suppression.

As can be seen in all columns of Table II, the majority of interaction energies of ^{3}H and ^{4}He comes from the tensor force in the triplet-even state. From Table III, it is clear that most of the interaction energy of deuteron is also due to the tensor force. The total contribution to the nuclear matter from tensor forces in the triplet-even and the triplet-odd state is given in parenthesis in Table IV, which is a considerable part of the interaction energy, too. In Fig. 6, the ratio of the tensor contribution to the total interaction energy,

$$\varepsilon_T = \langle \Psi | v_T | \Psi \rangle / \langle \Psi | v | \Psi \rangle , \tag{25}$$

is shown (v_T is the tensor part of v). The ratio ε_T shows the trend that the tensor suppression increases as the mass number increases.

The mass number dependence of both suppressions is the cause of the reversal of binding energy. The potential (R) works effectively for ^{3}H in getting the binding energy, because suppressions of its strong tensor force and its retarded part, both of which have attractive contributions, are small as compared to the ^{4}He case. On the other hand, in ^{4}He, these suppressions are so large that (R) is less effective than (NR) in getting the binding energy.

4.4. *Mechanism of the OES suppression*

The OES suppression depends on the mass number. To clarify the mechanism of OES suppression and its mass number dependence, we expand the matrix element

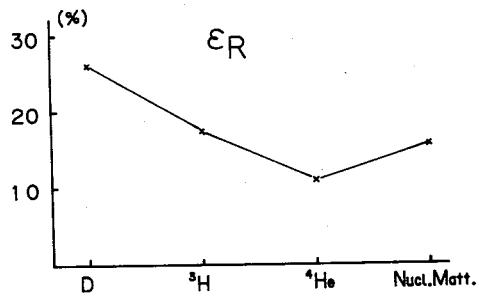

Fig. 5. The mass number dependence of the ratio ε_R (given by Eq. (24) in the text).

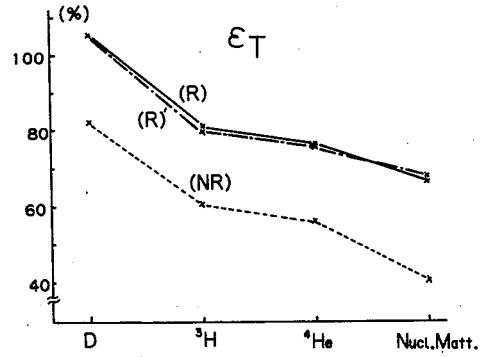

Fig. 6 The mass number dependence of the ratio ε_T (given by Eq. (25) in the text) for (R)(solid line), (NR)(dashed line) and (R)'(dash-dotted line).

$\langle\Psi|v(ij)|\Psi\rangle$ as follows:

$$\langle\Psi|v(ij)|\Psi\rangle=\langle\Phi|v(ij)|\Phi\rangle+\sum_{(kl)}\left\langle\Phi|v(ij)\frac{Q_{kl}}{e}v(kl)|\Phi\right\rangle$$

$$+\sum_{(kl,mn)}\left\langle\Phi|v(ij)\frac{Q_{kl}}{e}v(kl)\frac{Q_{mn}}{e}v(mn)|\Phi\right\rangle+\cdots. \tag{26}$$

Let us pay attention to the ratarded effects appeared in higher order terms beside the

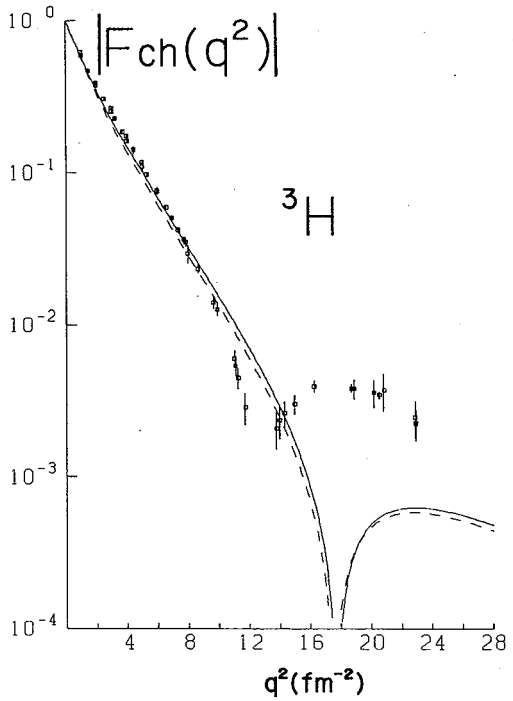

Fig. 7. Charge form factors of ^{3}H calculated by (R) (solid line) and (NR) (dashed line). The experimental values are taken from Ref. 10).

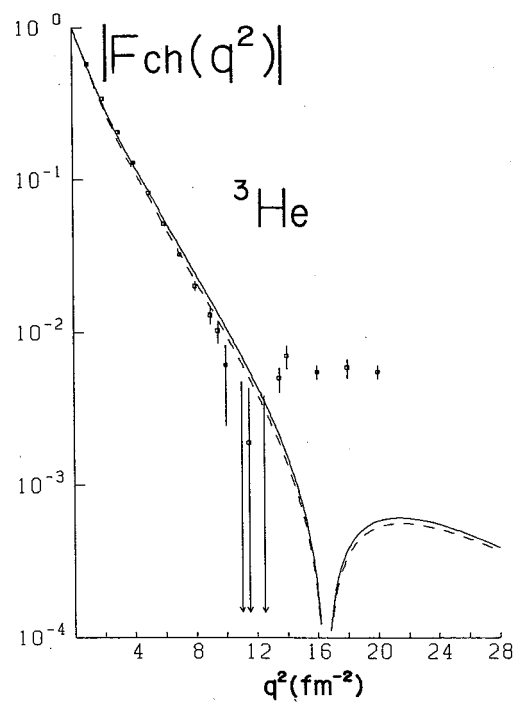

Fig. 8. Charge form factors of ^{3}He. The curves are the same as in Fig. 7. The experimental values are taken from Ref. 11).

first term of Eq. (26). Since they are related to the intermediate state, these effects are expected to be rather large and their magnitude depends on the energy denominator. In the deuteron, the energy denominator has small value because of the most loosely bound nucleus, so the OES contribution is the largest. On the other hand, in ^{3}H and ^{4}He, the energy denominators in the intermediate states get larger, because these nuclei are more and more tightly bound. Namely, the OES effect gradually decreases with increase of the mass number.

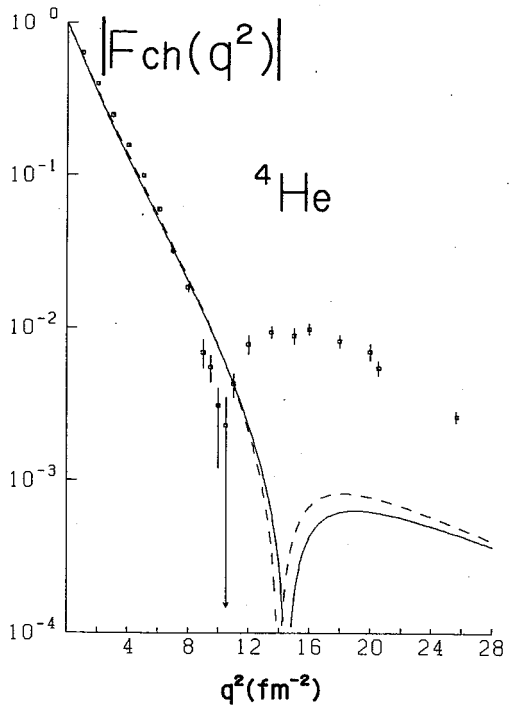

Fig. 9. Charge form factors of ^{4}He. The curves are the same as in Fig. 7. The experimental values are taken from Ref. 12).

4.5. *Charge form factors of ^{3}H, ^{3}He and ^{4}He*[2e]

Calculations with the impulse approximation for the charge form factors of ^{3}H, ^{3}He and ^{4}He are carried out by using the ATMS wave functions. The results are given in Figs. 7~9. Similar to other N-N potentials, the first minimums occur at larger values of q^2 than the experimental ones and the heights of the second maximum are too low. The differences between the calculations with (R) and (NR) are rather small. It is noted that both potentials have the Gaussian soft core and this property may explain the poor prediction at high momentum transfers.

§ 5. Summary and conclusion

We have calculated the binding energies of ^{3}H and ^{4}He with two kinds of the Funabashi potential, (R) and (NR). Results are compared with binding energies of deuteron and nuclear matter with the same potentials.

The tensor force of (R) is stronger than that of (NR). In addition, (R) incorporates the retardation which is the attractive OES interaction, but (NR) does not. The calculations have been performed by the ATMS method. This variational method is so skilful that we are able to analyze the energy contents of these systems in detail.

The charge form factors of ^{3}H, ^{3}He and ^{4}He are also calculated with the impulse approximation.

The results show that the binding energy of ^{3}H by (R) is larger than that by (NR), while the roles of (R) and (NR) are reversed in ^{4}He and the nuclear matter. The cause for this reversal can be traced back to the mass number dependence of the suppressions of the OES interaction and the tensor force in nuclei. Then the ^{3}H system is more sensitive to both the tensor force and the OES interaction than the

^{4}He system.

As mentioned in § 1, taking the three-body force into account, ^{3}H is slightly underbound but ^{4}He is overbound by a few MeV. Considering this situation, we may conclude that a N-N potential having an attractive OES interaction in addition to a strong tensor force in the triplet-even state is desirable.

Acknowledgements

The authors would like to express their thanks to Professor Y. Akaishi, Professor H. Tanaka and Professor M. Wada for valuable discussions and encouragements and to Dr. M. Sakai for his helpful comments to this work. The numerical computation was carried out at the Computer Center of Nihon University at Narashino.

References

1) J. A. Tjon, *The Few Body Problems*, ed. F. S. Levin (North-Holland, 1981), p.47.
2a) M. Sato, Y. Akaishi and H. Tanaka, Prog. Theor. Phys. Suppl. No. 56 (1974), 76; Prog. Theor. Phys. **66** (1981), 930.
b) Y. Akaishi, M. Sakai, J. Hiura and H. Tanaka, Prog. Theor. Phys. Suppl. No. 56 (1974), 6.
c) M. Sakai, I. Shimodaya, Y. Akaishi, J. Hiura and H. Tanaka, Prog. Theor. Phys. Suppl. No. 56 (1974), 32.
d) H. Tanaka and H. Nagata, Prog. Theor. Phys. Suppl. No. 56 (1974), 121.
e) T. Katayama, M. Fuyuki, Y. Akaishi, S. Nagata and H. Tanaka, Prog. Theor. Phys. Suppl. No. 56 (1974), 54.
T. Katayama, Y. Akaishi and H. Tanaka, Prog. Theor. Phys. **63** (1980), 2127; **67** (1981), 236.
f) H. Tanaka, Nucl. Phys. **A328** (1979), 454.
3) J. Carlson, V. R. Pandharipande and R. B. Wiringa, Nucl. Phys. **A401** (1983), 59.
4) J. Fujita and H. Miyazawa, Prog. Theor. Phys. **17** (1957), 360.
5) L. A. Kondratyuk, J. Vogelzang and M. S. Fanchenko, Phys. Lett. **98B** (1981), 59.
6) P. Sauer and J. A. Tjon, Nucl. Phys. **A216** (1973), 541.
7) T. Obinata and M. Wada, Prog. Theor. Phys. **53** (1975), 732.
8) T. Obinata, Prog. Theor. Phys. **73** (1985), 1270.
9) Y. Akaishi, Nucl. Phys. **A416** (1984), 409c.
10) H. Collard et al., Phys. Rev. **138** (1965), B57.
F. P. Juster et al., Phys. Rev. Lett. **55** (1985), 2261.
S. Platchkov, private communication.
11) J. S. McCarthy, I. Sick and R. R. Whitney, Phys. Rev. **C15** (1977), 1396.
12) R. F. Frosch et al., Phys. Rev. **160** (1967), 874.
R. G. Arnold et al., Phys. Rev. Lett. **40** (1978), 1429.